

## Off-lattice noise reduction and the ultimate scaling of diffusion-limited aggregation in two dimensions

Robin C. Ball,<sup>1</sup> Neill E. Bowler,<sup>1</sup> Leonard M. Sander,<sup>2</sup> and Ellák Somfai<sup>1,3</sup><sup>1</sup>*Department of Physics, University of Warwick, Coventry, CV4 7AL, England*<sup>2</sup>*Michigan Center for Theoretical Physics, Department of Physics, University of Michigan, Ann Arbor, Michigan 48109-1120*<sup>3</sup>*Instituut-Lorentz, Universiteit Leiden, Niels Bohrweg 2, 2333 CA Leiden, The Netherlands*

(Received 16 August 2001; published 19 August 2002)

Off-lattice diffusion-limited aggregation (DLA) clusters grown with different levels of noise reduction are found to be consistent with a simple fractal fixed point. Cluster shapes and their ensemble variation exhibit a dominant slowest correction to scaling, and this also accounts for the apparent “multiscaling” in the DLA mass distribution. We interpret the correction to scaling in terms of renormalized noise. The limiting value of this variable is strikingly small and is dominated by fluctuations in cluster shape. Earlier claims of anomalous scaling in DLA were misled by the slow approach to this small fixed point value.

DOI: 10.1103/PhysRevE.66.026109

PACS number(s): 64.60.Ak, 61.43.Hv

### I. INTRODUCTION

Since its introduction in 1981, the diffusion-limited aggregation (DLA) model of Witten and Sander [1] has been a paradigm of self-organized scaling behavior in irreversible growth. However, even after more than 20 years, there is still controversy about its scaling properties; many authors have claimed, for example, that DLA clusters do not scale as simple fractals, but instead have various anomalous features. In this paper we give data on DLA clusters with noise reduction, which enables us to refute conclusively the basis of these claims of anomalous scaling. We will show that the apparent anomalies arise from a slowly decaying correction to scaling which can be associated with the level of intrinsic growth fluctuations, as suggested in Ref. [2]. The analysis of these corrections to scaling gives us considerable insight into the asymptotic behavior of DLA, i.e., the DLA fixed point.

In (off-lattice) DLA a cluster is rigid and stationary, growing from one seed particle by accretion at first contact of  $N$  mobile diffusing hard sphere particles. The diffusing particles are sufficiently dilute so that they can be taken to arrive one at a time. We consider the distribution of where growth (by deposition) occurs at a given cluster size. The average radius of deposition is defined by  $R_{\text{dep}} = \langle r \rangle$ , where  $r$  is the distance of deposition from the center of the cluster. There is no controversy that  $R_{\text{dep}} \propto N^{1/D}$ , consistent with a simple fractal of dimension  $D = 1.71$  for large clusters in two dimensions. However the spread of the deposition radius is thought to show anomalies. Plischke and Rácz [3] introduced the penetration depth,  $\xi$ , the standard deviation of radius of deposition of a given cluster, and claimed that it scaled differently from  $R_{\text{dep}}$ . More recently, Davidovitch *et al.* [4] considered the standard deviation of the cluster average radius across the ensemble of clusters,  $\delta R_{\text{eff}}$ , and claimed that it was asymptotically negligible compared to the mean. Another anomalous feature that has been claimed of DLA is multiscaling [5,6]: the fractal dimension of the cluster is said to depend on the distance (relative to the cluster radius) from the center. We will examine these claims using finite size scaling with the help of noise reduction and show that none

of them hold. We find that DLA is consistent with simple scaling, and the apparently anomalous scaling can all be explained by a slow correction to scaling.

### II. OFF-LATTICE NOISE REDUCTION

Noise reduction for the *lattice version* of DLA has been introduced [7,8] with the aim of suppressing the shot noise of the individual incoming particles. When growing at lower noise levels, the clusters achieve more asymptotic behavior at smaller sizes: a prime example of this is that the lattice effects show up earlier. These lattice effects on noise-reduced clusters (or without noise reduction on very large clusters) are quite strong, so in order to avoid them, any analysis of large scale DLA clusters has to be made off-lattice.

In our version of noise-reduced off-lattice DLA the particles diffuse freely until they contact a particle in the cluster, just as in the original model. However, on contact with a particle of the existing cluster, the diffusing particle is moved into that particle by a factor of  $A$ , at which point it is irreversibly stuck (see Fig. 1). This means that shallow bumps are added to the cluster, and that we must add  $1/A$  particles on top of one another to protrude the growth by a particle diameter. A cluster grown with this method of noise reduction is shown in Fig. 2. Another way to do noise reduction of this type was introduced by Stepanov and Levitov [9], who

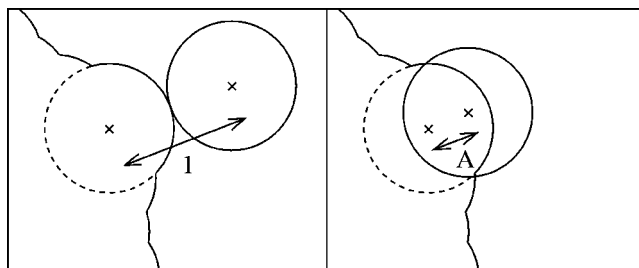


FIG. 1. The noise-reduced DLA algorithm. A particle is allowed to diffuse freely until it contacts a cluster particle. The diffusing particle is moved onto the cluster particle, reducing the distance between their centers by a factor  $A$ .

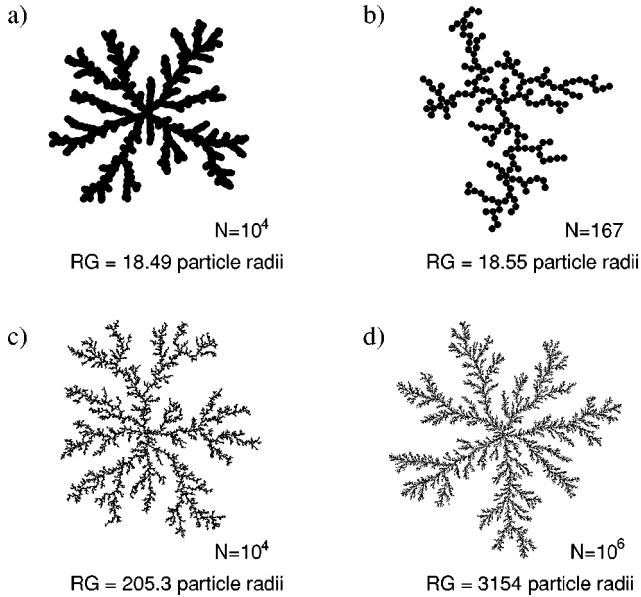


FIG. 2. Cluster (a) grown with noise reduction  $A = 0.03$  is compared with clusters grown without noise reduction,  $A = 1$ : (b) has same gyration radius, (c) has same number of particles, and (d) has same correction-to-scaling properties (e.g., relative penetration depth). The numbers shown are the particle number and gyration radius.

generalized the method of iterated conformal maps [10,4] to add shallow bumps.

### III. FINITE SIZE SCALING

Growing clusters at a variety of levels of noise reduction gives us a very clear picture of the finite size scaling effects in DLA. We grew 1000 DLA clusters to 1 000 000 particles with noise reduction levels of  $A = 0.3, 0.1, 0.03, 0.01$ , and 4000 clusters with  $A = 1$  as well as 25 clusters with  $A = 0.001$ . At various points in the growth, 100 000 probe particles were fired at each cluster to measure its properties. In the following measurements the center of the cluster was taken naturally as the center of mass of these probe particles (i.e., center of charge).

Figure 3 shows a primary test of scaling: how the relative penetration depth, the ratio of penetration depth to mean radius of deposition  $\Xi \equiv \xi/R_{\text{dep}}$ , varies with  $N$ . The different levels of noise reduction are all consistent with a universal asymptote,  $\Xi_{\infty} \approx 0.12$ , and with  $N^{-0.33}$  as the common correction to scaling at large  $N$ . Figure 3 also shows data obtained with the Hastings and Levitov (HL) iterated conformal map method [10]. We can make a naive geometric argument to see how the HL bumps correspond to different levels of off-lattice noise reduction. In the HL method the bumps are generated by a conformal map parametrized by  $a$  (see Ref. [10] for details), with small  $a$  giving shallow bumps. Using the scheme of Fig. 1, and working out when the aspect ratios of the two types of bumps match, we find  $(1/a - 1)^2 = 2/A - 1$ . Thus  $a = 0.5$  corresponds to ordinary DLA. Other equivalent cases are indicated in the legend of Fig. 3, showing that this naive argument represents reason-

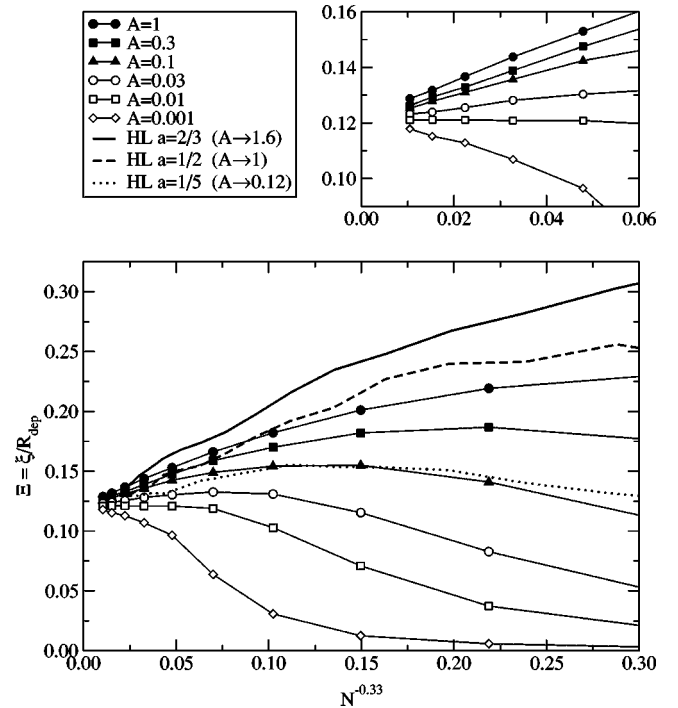


FIG. 3. Behavior of the relative penetration depth  $\Xi = \xi/R_{\text{dep}}$ , with varying cluster size at various levels of noise reduction. The abscissa is chosen according to the correction to scaling exponent measured from Fig. 4. The relative penetration depth clearly converges to a nonzero common value. Also shown are curves for clusters grown by the Hastings-Levitov (HL) method with expected equivalence indicated in the legend. The top right panel is a magnification of the asymptotic end of the curves.

ably well the relationship between our noise reduction and that of Ref. [9].

The correction-to-scaling exponents we report in this paper are not arbitrary fits, but directly measured as follows. If we posit a leading asymptotic form of some quantity,  $Q$ ,

$$Q(N) = Q_{\infty}(1 + CN^{-\nu}), \quad (1)$$

then a plot of  $dQ(N)/d \ln(N)$  vs  $Q(N)$  should have an intercept on the  $Q$  axis of  $Q_{\infty}$  approached with slope  $-\nu$ , both independent of the magnitude of  $C$ . Figure 4 shows this analysis applied to  $\Xi$  and this is the basis for the choice of exponent  $\nu = 0.33$  for Fig. 3. This provides unbiased evidence that all the different levels of noise-reduction approach the same asymptotic value  $\Xi_{\infty}$ , consistent with a common correction to scaling exponent. Interestingly the “fixed point” can be approached from either side, corresponding to opposite signs of  $C$ .

A deeper test of the universality of these clusters and their scaling comes from the multipole moments of the growth probability distribution. The  $n$ th multipole moment is given by

$$M_n = \int dq(x + iy)^n, \quad (2)$$

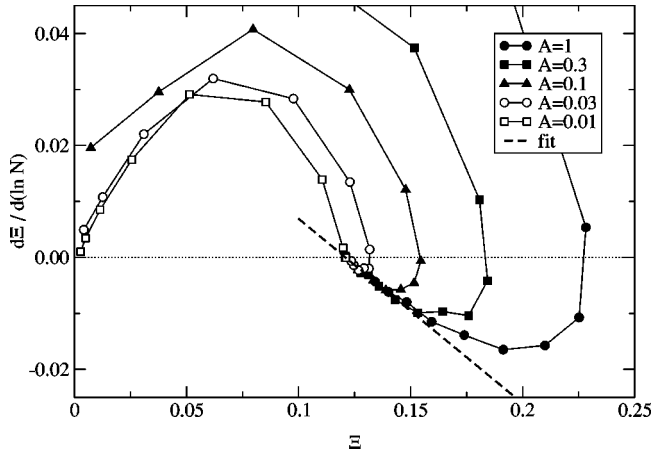


FIG. 4. Rate of change of the relative penetration depth  $d\Xi/d \ln(N)$  plotted against  $\Xi$ . The common dashed asymptote indicates that  $\Xi$  has a dominant correction to scaling of the form  $\Xi = \Xi_\infty(1 + CN^{-\nu})$  with  $\Xi_\infty = 0.121 \pm 0.003$  from the intercept of the plots and  $\nu = 0.33 \pm 0.06$  from the slope.

where  $q$  is the probability distribution for where growth will next occur. (Note that  $q$  is equivalent to the charge density on the cluster surface when it is considered to be a conductor held at a fixed potential.) The multipole moments for positive  $n$  fully characterize the cluster shape, and can be related invertibly to the Laurent coefficients of its conformal map from the unit circle [4]. In practice we measured the  $M_n$  by sampling  $(x + iy)^n$  with nongrowing probe particles.

Figure 5 shows the correction-to-scaling analysis of the corresponding multipole powers

$$P_n = \frac{|M_n|^2}{R_{\text{eff}}^{2n}}, \quad (3)$$

where we have scaled each  $M_n$  by the appropriate power of the effective (or Laplace [4]) radius,  $R_{\text{eff}}$ , which is given by  $\ln R_{\text{eff}} = \int dq \ln(r)$ . Each of  $P_2$ – $P_5$  is consistent with a universal nonzero asymptote, and moreover they are all compatible with a single common correction-to-scaling exponent 0.33, see Table I. Figure 6 collects the resulting finite size scaling plots assuming this exponent. Together with the relative penetration depth results, this presents strong evidence for universal asymptotic geometry for DLA clusters, and a universal leading correction-to-scaling exponent  $\nu = 0.33$ .

In all of the measurements discussed above, the cluster center used was the center of charge, natural to a snapshot of the growth. In the following section, however, we will require to compare data at different cluster sizes where it becomes natural to use a fixed center, namely the cluster “seed.” Accordingly we have also measured the finite size scaling of various lengths with the seed as fixed origin, and in all cases using direct ensemble averages and for clusters with no noise reduction ( $A = 1$ ). Using the seed as center also naturally leads to the measurement of penetration depth as the rms spread of deposition radius about its ensemble average,

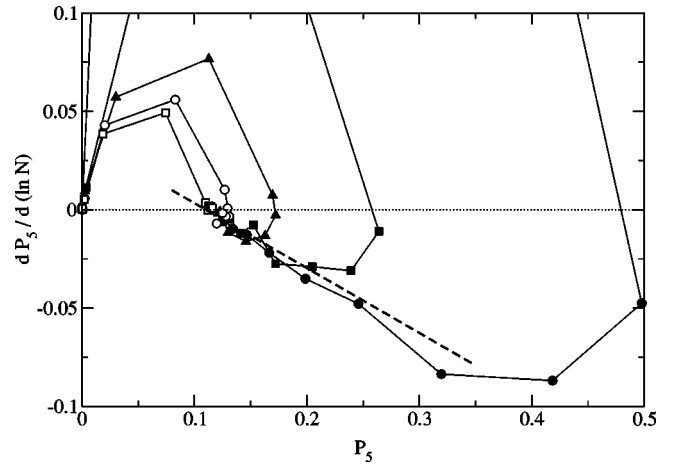
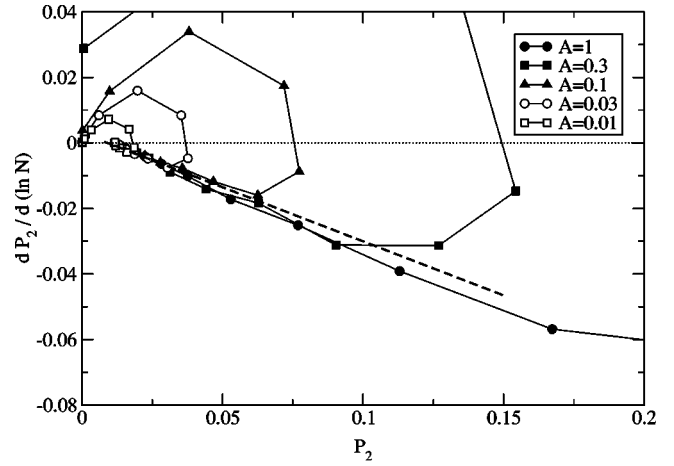


FIG. 5. The rate of change of the multipole powers  $P_2$  and  $P_5$  with respect to  $\ln(N)$  against the multipole powers. Each show a correction to scaling exponent of 0.33 (dotted lines), within statistical error.

$$\xi_0 = \sqrt{\langle r^2 \rangle - \langle r \rangle^2}, \quad (4)$$

rather than computing the variance cluster-by-cluster before averaging, i.e.,

$$\xi = \sqrt{\left\langle \left( \int dq r^2 - \left( \int dq r \right)^2 \right) \right\rangle}. \quad (5)$$

Figure 7 shows the fits of the following form:

$$R(N) = \hat{R} N^{1/D} (1 + \tilde{R} N^{-\nu}), \quad (6)$$

and the coefficients are collected in Table II.

It is worth noting that the effect of changing the center is negligible except perhaps for the penetration depth, where

TABLE I. Best fit scaling exponents for  $P_2$ – $P_5$ . We have also measured  $P_6$ – $P_{10}$ . These yield somewhat larger apparent exponents with large statistical errors.

	$P_2$	$P_3$	$P_4$	$P_5$
$\nu$	$0.41 \pm 0.08$	$0.27 \pm 0.06$	$0.41 \pm 0.12$	$0.40 \pm 0.12$

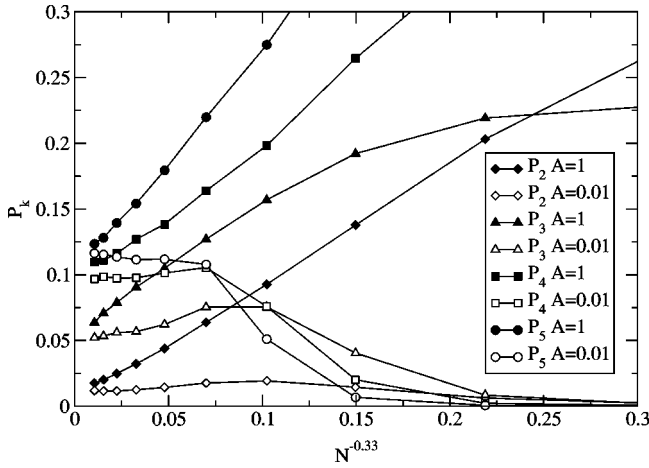


FIG. 6. Finite size scaling plots for  $P_2$ – $P_5$  for  $A=1$  and  $A=0.01$ . All the multipole powers exhibit the same correction-to-scaling exponent.

for  $\xi$  using the center of charge (as for Figs. 3 and 4), the coefficients are  $\hat{\xi}=0.089$  and  $\tilde{\xi}=5.8$  as opposed to those shown for  $\xi_0$  in Table II.

#### IV. MULTISCALING

Now we consider the anomalous scaling claim of multiscaling, when the aggregate has a fractal dimension that depends upon the distance from the seed as a fraction of cluster radius. It was proposed in Ref. [5] that the ensemble average of the density of particles  $g_N(r)$  of an  $N$ -particle cluster at distance  $r$  away from the seed obeys

$$g_N(xR_{\text{gyr}}) = A(x)R_{\text{gyr}}^{-d+D(x)}, \quad (7)$$

where the dimension  $D(x)$  is function of  $x=r/R_{\text{gyr}}$ , and the size  $N$  and (average) radius of gyration  $R_{\text{gyr}}$  are, of course, mutually dependent. Using the above formula at fixed  $x$ , one can extract the dimension  $D(x)$  by the scaling with  $R_{\text{gyr}}$ ,

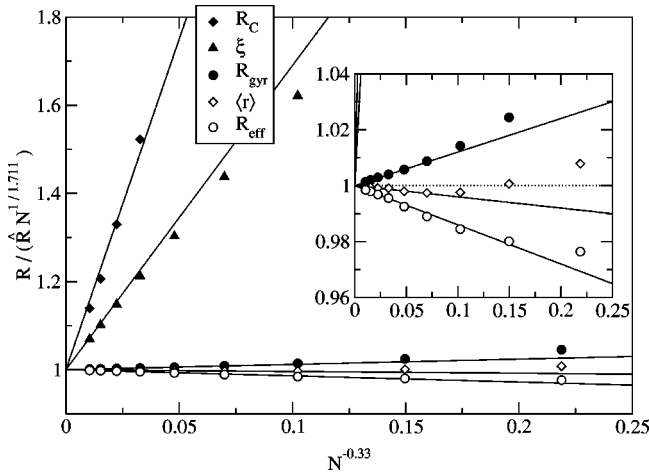


FIG. 7. Correction-to-scaling plots of various quantities of dimension length (without noise reduction,  $A=1$ ). The largest correction is obtained by the penetration depth  $\xi$ . The inset magnifies the y axis around 1.

TABLE II. Coefficients of correction-to-scaling fits of form Eq. (6), with  $D=1.711$  and  $\nu=0.33$ . The various lengths are radius of deposition  $R_{\text{dep}}=\langle r \rangle$ , seed to center of charge distance  $R_C = \sqrt{\langle |f d q \mathbf{r}|^2 \rangle}$ , effective radius  $R_{\text{eff}} = \exp\langle \ln r \rangle$ , gyration radius  $R_{\text{gyr}} = \sqrt{1/N \sum_{N'=1}^N \langle r^2 \rangle_{N'}}$ , and ensemble penetration depth  $\xi_0 = \sqrt{\langle r^2 \rangle - \langle r \rangle^2}$ , where the averages are over the ensemble of clusters at fixed  $N$ .

	$R_{\text{dep}}$	$R_C$	$R_{\text{eff}}$	$R_{\text{gyr}}$	$\xi_0$
$\hat{R}$	0.733	0.027	0.726	0.501	0.091
$\tilde{R}$	-0.04	15	-0.14	0.12	6.9

$$-d + D(x) = \left. \frac{\partial \ln g_N(xR_{\text{gyr}})}{\partial \ln R_{\text{gyr}}} \right|_x = \frac{R_{\text{gyr}}}{dR_{\text{gyr}}/dN} \left. \frac{\partial \ln g_N(xR_{\text{gyr}}(N))}{\partial N} \right|_x. \quad (8)$$

Simple fractal scaling would require  $D(x)=D$  independent of  $x$ , but the dimension measured this way in Ref. [6] using medium size clusters ( $N=10^4$ – $10^5$ ) was observed to be a nontrivial function (see Fig. 8). Others partly confirmed that findings, although with mixed results [11,12].

Now we will repeat the same measurement procedure but instead of a direct simulation we use the correction-to-scaling results of the preceding section, within a scaling function assumption (see below). This turns out to agree quantitatively with the earlier published  $D(x)$  data, but implies that the ultimate behavior is simple fractal scaling with  $D(x) \rightarrow D$  for all  $x$ .

Consider the distribution of  $r$ , the distance of attaching particles from the seed: as we have seen, this has mean  $R_{\text{dep}}$  and variance  $\xi_0$ . Now we assume that the *shape* of the probability density function is independent of  $N$ ,

$$\frac{1}{\xi_0(N)} h\left(\frac{r - R_{\text{dep}}(N)}{\xi_0(N)}\right), \quad (9)$$

where  $h$  is a normalized probability density with zero mean and unit variance. After replacing the sum over particles with an integral, for the particle density we get

$$2\pi r g_N(r) = \int_0^N \frac{dN'}{\xi_0(N')} h\left(\frac{r - R_{\text{dep}}(N')}{\xi_0(N')}\right). \quad (10)$$

A similar formula has been suggested in Ref. [13]. Given that we have already studied  $R_{\text{dep}}(N)$ ,  $R_{\text{gyr}}(N)$ , and  $\xi_0(N)$ , the only outstanding quantity to be found is the scaling function  $h$ , which we find to be very close to the standard normal distribution, see Fig. 9.

Figure 8 shows how well  $D(x)$  derived from our finite size scaling results and a normal distribution for  $h$  agrees with the raw data of Ref. [6]. Also shown is what our results imply for the behavior at larger  $N$ , and as  $N \rightarrow \infty$  with  $R_{\text{dep}}$ ,  $R_{\text{gyr}}$ , and  $\xi_0$  approaching pure scaling,  $D(x) \rightarrow D$ . Thus we conclude that all the apparent reported  $x$  dependence of  $D(x)$  arises from corrections to scaling, and indeed almost all the

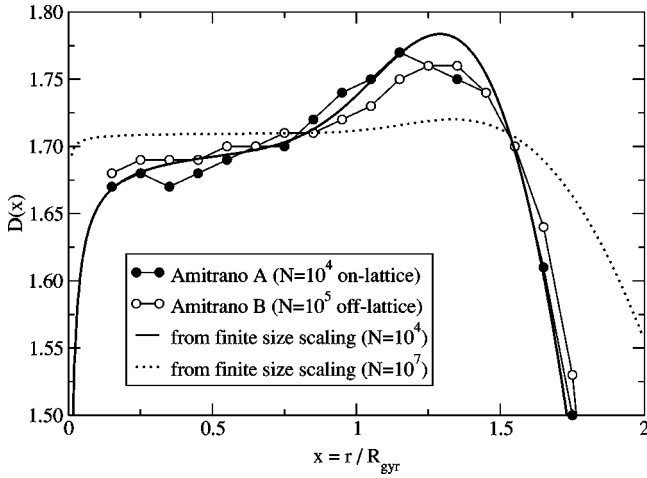


FIG. 8. Comparison of “multiscaling dimensions” from Ref. [6] and the finite size scaling prediction discussed in the text. The finite size scaling prediction implies that as  $N \rightarrow \infty$ ,  $D(x) \rightarrow D$  for all  $x$ , and the predicted approach at  $N = 10^7$  is shown. The only inputs to the finite size scaling curves are  $R_{\text{dep}}$ ,  $R_{\text{gyr}}$ , and  $\xi_0$  using Eq. (6) with parameters from Table II, and a Gaussian model for the scaling function (see Fig. 9).

effect comes from the relatively large corrections to scaling in  $\xi_0$ . Our interpretation of this data also resolves a previously noted paradox [6], namely, that  $D(x)$  increasing with  $x$  cannot be asymptotic scaling as it would imply some decrease of  $g_N(r)$  with increasing  $N$  at fixed  $r$ .

## V. SIZE FLUCTUATIONS AND FIXED POINT

We now present an interpretation of the leading correction to scaling, based on observations from our data and building on earlier work [8]. The amplitude of the leading correction to scaling crosses zero at a common value of noise reduction  $A_f \approx 0.01$ , for *all* of the plots in Figs. 3 and 6. This suggests that the noise reduction and the correction to scaling are

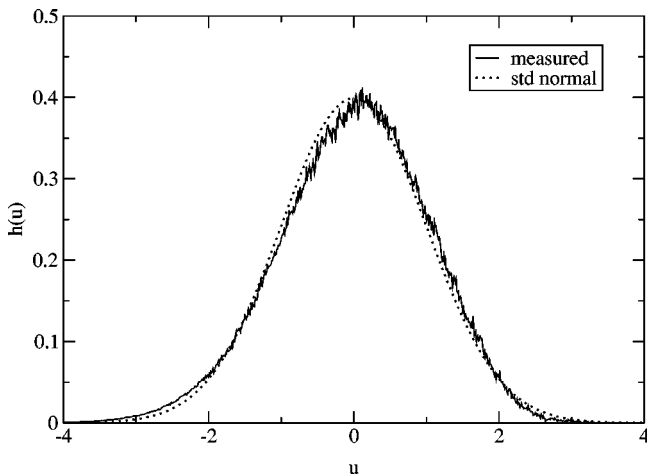


FIG. 9. The scaling function  $h$ . The measured data at  $N = 10^4$  (continuous line) are compared to standard normal distribution (smooth dotted line). For the measurement, the histogram bin width was  $\Delta u = 0.01$ .

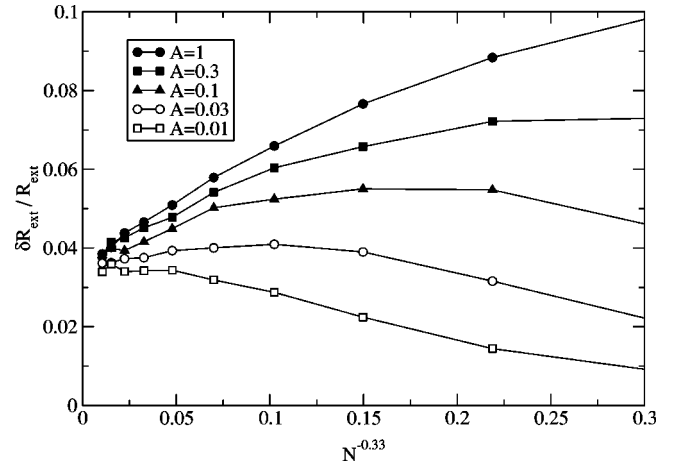


FIG. 10. Ensemble spread of extremal cluster radius, which tends to the value  $0.035 \pm 0.003$ .

fundamentally related, which can be understood by using the renormalization theory of noise reduction of Barker and Ball [8]. In this view, the cluster is approximated as being at its large  $N$  fixed point if one unit of growth acts as a coarse graining of DLA on finer length scales. This seems to occur if we grow with input noise near  $A_f$ . This is equivalent to having  $\delta N/N = \sqrt{A_f}$  for relative fluctuation in the number of particles to advance the growth locally by one particle diameter.

We can also view this in terms of a fixed point for the noise output of the growth,  $\sqrt{A_{\text{out}}} = \delta N/N$ , in terms of the relative fluctuation in the number of particles to span a fixed radius. Figure 10 shows our data for the ensemble spread of extremal cluster radius. Since this spread is small, we can infer

$$\left. \frac{\delta N}{N} \right|_{R_{\text{ext}}} = D \left. \frac{\delta R_{\text{ext}}}{R_{\text{ext}}} \right|_N = 0.060 \pm 0.005 \quad (11)$$

from our extrapolated value. Thus we find an asymptotic renormalized noise  $A^* = 0.0036 \pm 0.0006$ . This is in qualitative agreement with our observed value of  $A_f$ . Furthermore, Fig. 11 shows how well this vindicates Barker and Ball’s earlier estimates of the fixed point, using our value of  $\nu$  to extrapolate from their finite size calculations. By contrast, the more recent work of Cafiero *et al.* [14] using a very small scale renormalization scheme disagrees by two orders of magnitude.

Our interpretation is thus that the renormalized noise is the slow variable that dominates convergence of other quantities to scaling. Our observed input noise value of  $A_f \approx 10^{-2}$  (for the leading correction to scaling to vanish) and the extrapolated fixed point output noise  $A^*$  are equal within a factor of order unity, showing the consistency of the picture.

We can take this interpretation a step further to infer that the dominant fluctuations of  $R_{\text{ext}}$  determining the noise reduction are fluctuations in cluster shape rather than overall cluster radius. The basis for this is that the logarithmic average radius,  $R_{\text{eff}}$ , has much smaller spread, asymptotically

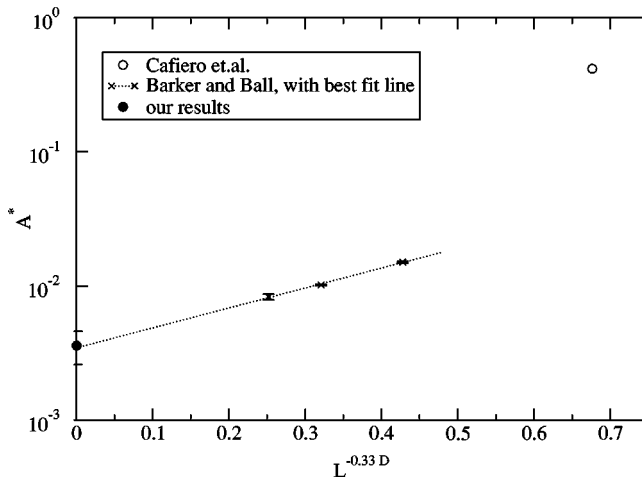


FIG. 11. Estimate of the fixed point value of  $A$  ( $A^*$ ), combined with previous estimates from Barker and Ball (the middle three points) and Cafiero (the rightmost point). The Barker and Ball data are in good agreement with our results, but the Cafiero data disagree.

$\delta R_{\text{eff}}/R_{\text{eff}}=0.012 \pm 0.001$  compared to  $\delta R_{\text{ext}}/R_{\text{ext}}=0.035 \pm 0.003$ . Since  $R_{\text{eff}}$  is an average that emphasizes typical size, the larger fluctuations in  $R_{\text{ext}}$  which gave us  $A^*$  must be attributed to shape. (However, we showed in Ref. [2] that  $R_{\text{eff}}$  has the same crossover exponent,  $\nu$ , as the other quantities discussed here.) In this sense DLA clusters are fundamentally stochastic objects with a distribution of shape.

## VI. SUMMARY

We believe our work opens the way to a definitive view of DLA in two dimensions, and the extension of this work to three dimensions is in hand. The identification of “DLA fixed point behavior” is now reasonable, as we have shown the sort of universal limiting amplitudes and correction-to-scaling exponents associated with such terminology.

Some main areas are outstanding. First, the renormalized

noise,  $\delta N/N = \sqrt{A^*}$ , is not of order unity, as we might expect *a priori*, and as has been suggested [14]. We do not understand the origin of this small number, and tracing its origin is a central remaining challenge in understanding DLA. Another puzzle that we hope to address in a later paper is why the fractal dimension is comparatively insensitive to the convergence of the renormalized noise.

Also, we need to understand the full scaling of the probability distribution for growth in DLA, corresponding to the harmonic measure of the perimeter. To this end the more expensive cluster growth methods of HL [10] are likely to come into their own as they yield the harmonic measure directly. Stepanov and Levitov [9] have already shown some results for HL clusters grown with shallow bumps, corresponding rather closely to our noise-reduction technique.

The richer, simpler area to explore is the response to anisotropy and its sensitivity to noise. Small DLA clusters appear robust to the intrinsic bias of growing on a square lattice, whereas large clusters (and equivalently noise reduced ones) are driven to grow a four-fingered dendrite. The first requirement is a systematic analysis of how this is a relevant perturbation of the isotropic DLA fixed point. Second, we might ask whether the anomalous response for small simple DLA clusters is dominated by some other hitherto unsuspected fixed point with much larger noise level. There is another rather neglected nearby fixed point, that of spherical growth, which becomes more pertinent at high noise reduction—where it takes longer to exhibit its instability. We suggest that the influence of this fixed point may be responsible for shifting the observed  $A_f$  somewhat above  $A^*$ , and this should be relatively amenable to analytic theory.

## ACKNOWLEDGMENTS

NEB would like to thank BP Amoco and EPSRC for the support during this research. E.S. was supported by the Dutch FOM Foundation and EC Grant No. HPMF-CT-2000-00800. We thank Paul Meakin and Thomas Rage for sending us a computer code that was used for some of the results presented here.

- 
- [1] T.A. Witten and L.M. Sander, Phys. Rev. Lett. **47**, 1400 (1981).
  - [2] E. Somfai, L.M. Sander, and R.C. Ball, Phys. Rev. Lett. **83**, 5523 (1999).
  - [3] M. Plischke and Z. Rácz, Phys. Rev. Lett. **53**, 415 (1984).
  - [4] B. Davidovitch, H.G.E. Hentschel, Z. Olami, I. Procaccia, L.M. Sander, and E. Somfai, Phys. Rev. E **59**, 1368 (1999).
  - [5] A. Coniglio and M. Zannetti, Physica A **163**, 325 (1990).
  - [6] C. Amitrano, A. Coniglio, P. Meakin, and M. Zannetti, Phys. Rev. B **44**, 4974 (1991).
  - [7] C. Tang, Phys. Rev. A **31**, 1977 (1985).
  - [8] P.W. Barker and R.C. Ball, Phys. Rev. A **42**, 6289 (1990).
  - [9] M.G. Stepanov and L.S. Levitov, Phys. Rev. E **63**, 061102 (2001).
  - [10] M.B. Hastings and L.S. Levitov, Physica D **116**, 244 (1998).
  - [11] P. Ossadnik, Physica A **176**, 454 (1991).
  - [12] P. Ossadnik, Physica A **195**, 319 (1993).
  - [13] J. Lee, S. Schwarzer, A. Coniglio, and H.E. Stanley, Phys. Rev. E **48**, 1305 (1993).
  - [14] R. Cafiero, L. Pietronero, and A. Vespignani, Phys. Rev. Lett. **70**, 3939 (1993).